

NURBS-based Inverse Reflector Design

Oscar Anson, Francisco J. Seron and Diego Gutierrez

University of Zaragoza

Abstract

Commonly used direct rendering techniques simulate light transport for a complete scene, specified in terms of light sources, geometry, materials, participating media, etc. On the other hand, inverse rendering problems take as input a desired light distribution and try to find the unknown parts of the scene needed to get such light field. The latter kind, where inverse reflector design is included, is traditionally solved by simulation optimization methods, due to the high complexity of the inverse problem. In this paper we present an inverse reflector design method which handles surfaces as NURBS and simulates accurately the light transport by means of a modified photon mapping algorithm. The proposed method is based on an optimization method, called pattern search, in order to compute the reflector needed to generate a target near light field. Some assumptions are determined in order to reduce the complexity of the problem, such as a rotationally symmetric reflector or its perfectly specular reflective behavior. The optimization method specifies the reflector shape by handling a NURBS curve as a generatrix, sequentially modifying the position and weights of its control points in order to obtain the reflector solution. Areas of applications of inverse reflector design span from architectural lighting design to car headlamps design.

Categories and Subject Descriptors (according to ACM CCS): I.3.7 [Computer Graphics]: Three-Dimensional Graphics and Realism

1. Introduction

Inverse rendering problems differ from traditional direct rendering techniques in the direction of the data flow during the computation process. While direct techniques compute the light transport from a completely specified three dimensional scene, the inverse process starts with a desired light distribution and tries to find the unknown information of the rendering equation such as geometry, materials, light sources, etc.

The rendering equation [Kaj86] can be rewritten in its compact form [Arv95] [Mar98] as follows

$$L = L_e + \hat{K}\hat{G}L \quad (1)$$

where L_e stands for the initial light introduced in the system (emitted light), \hat{K} is an operator that describes how surfaces reflect light (materials), \hat{G} indicates how light travels among surfaces (geometry) and L is the light reflected from surfaces. According to the type of unknown information in (1), a classification of inverse rendering problems was given

by Patow and Pueyo [PP03] (see Table 1). Our work falls in the subgroup of inverse geometry problems, where the unknown \hat{G} in (1) is the shape of a reflector surface of an optical set (a luminaire), modeled as a rotationally symmetric surface by handling a NURBS curve generatrix. Inverse geometry problems and methods have a high importance in industrial lighting design (car headlights, street lamps, architectural indoor lighting design, etc.).

Table 1: Classification of Inverse Rendering problems (after Patow and Pueyo [PP03]). Question marks stand for unknown information, check marks stand for known information. Asterisk superscript stands for partially known information.

	L	L_e	\hat{K}	\hat{G}
Direct rendering	?	✓	✓	✓
Inverse lighting	✓*	?	✓	✓
Inverse reflectometry	✓*	✓	?	✓
Inverse combined problems	✓*	?	?	✓
Inverse geometry	✓	✓	✓	?

Additionally, the nature of the solving algorithm applied to retrieve the unknown information leads to another taxonomy [LJPP06]. On one hand, direct-solving approaches avoid to solve the rendering equation by building the inverse problem as a system of equations. On the other hand, indirect-solving algorithms are based in optimization methods, which require evaluating the traditional direct rendering problem at each iteration. This paper takes the latter strategy in order to perform the inverse reflector design by means of a pattern search optimization algorithm.

This paper presents as main contributions an inverse reflector design method, by means of handling the representation of a rotationally symmetric reflector with a NURBS curve generatrix [PT97], simulating the light transport with a modified photon mapping technique [Jen01] and optimizing the design process with the pattern search algorithm of Hooke and Jeeves [HJ61].

The remainder of this paper is organized as follows: Section 2 presents previous work on the inverse rendering and inverse geometry fields. Section 3 puts forward a theoretical background on optimization. In Section 4 the inverse design method is developed. The paper ends with the results in Section 5 and conclusions and future work in Sections 6 and 7.

2. Related Work

Solving an inverse rendering problem is a task that usually either relies on a theoretical approach or tries to apply a numerical solution [LJPP06].

Ramamoorthi and Hanrahan introduced in [RH01] a signal-processing framework which describes the reflected light field as a convolution of the lighting and the Bidirectional Reflectance Distribution Function (BRDF), and expresses it mathematically as a product of spherical harmonic coefficients of the BRDF and the lighting. By viewing inverse rendering as a deconvolution, the authors showed why inverse rendering problems are ill-conditioned when soft shading features are present; which was previously observed by Marschner and Greenberg [MG97]. While in Ramamoorthi and Hanrahan's work [RH01] lighting is assumed to come from infinity and occlusion is ignored, Durand et al. [DHS*05] overcome these limitation, considering complex blockers and light transport by taking into account angular and spatial variation. Recently, Ramamoorthi and Hanrahan [RH01] developed a full gradient analysis of the basic shading steps, showing the relationship between spatial, and angular effects.

Early works on inverse geometry had restrictive assumptions on ray reflections, such as the one by Wescott and Norris [WN75]. More recent works by Wang [Wan96] and Oliker [Oli08] overcome this limitation. While the work by Wang introduced the design of reflectors assuming distant sources (a far field problem) and differential geometry formulation, Oliker presented a near field formulation with ro-

tationally symmetric reflectors. Numerical approaches, generally make use of spline-based surfaces and polygons to model the desired reflector together with an optimization method to find the shape. In this sense, Neubauer [Neu94] found a B-spline reflector by applying a Powell optimization method. Other authors used Genetic Algorithms to overcome the problem of minimizing the nonlinear problem in inverse surface design, such as Doyle et al. [DCC99] and Choi et al. [CKP*07]. Doyle et al. [DCC99] performed a computer simulation, consisting of a 2D optical reflector modeled using a Bezier curve with a point light source. They compute light distributions in the near, middle and far fields using a ray-tracing approach, automating the design process through the use of a differential evolutionary strategy. Similarly, Choi et al. [CKP*07] introduce a design method of dome pendant prismatic luminaires by means of a micro genetic algorithm. Finally, Patow et al. [PPV04] proposed a technique for the design of reflector surfaces from a desired far field radiance distribution and geometrical constraints imposed by industry needs. They proposed a regular grid structure for the representation of the reflector surface and Monte Carlo light tracing for the computation of radiance transport.

In this paper we propose a method for inverse designing rotationally symmetric reflectors given a desired near field irradiance distribution. Our proposed method differs from previous work in the following ways:

- The representation of the rotationally symmetric reflector is based on a NURBS curve generatrix. We choose this representation due to two reasons. First, the use of this approach, instead of a polygon mesh (as in Patow et al. [PPV04]), drastically reduces the dimension of the optimization problem. Second, NURBS curves are widely used in CAD applications and industrial design. The use of NURBS, instead of B-splines (such as Neubauer [Neu94]), also gives more flexibility designing shapes due to the extra parameter to handle the weight of each control point.
- We use traditional photon mapping [Jen01] in order to solve the rendering equation, thus accurately simulating inter-reflections and caustics generated by the reflector. We introduce a modification in the photon storing procedure, just storing the particles which interact with the near field of study, allowing to store more photons for a more accurate irradiance estimate. As opposed to the work of Doyle et al. [DCC99], we perform a 3D physically-based global illumination simulation.
- We use the pattern search algorithm from Hooke and Jeeves [HJ61] in order to find the optimal reflector shape. This kind of direct searches tries to guess patterns of ever-improving solutions in order to reduce the number of expensive evaluations of the objective function.

3. Optimization

Inverse rendering, and hence inverse reflector design, can be seen as a type of mathematical problem, usually called optimization. Optimization can be defined as the process of finding the conditions that give the maximum or minimum value of a function. Therefore, an optimization problem can be stated as follows

$$\min_{\vartheta \in \Omega} f(\vartheta), \quad \text{with } \Omega \subseteq \mathbf{R}^n \quad (2)$$

where $\vartheta \equiv (\vartheta_1, \dots, \vartheta_n)$ is a n -dimensional vector in \mathbf{R}^n , called the *decision variable*, $f: \mathbf{R}^n \rightarrow \mathbf{R}$ is termed the *objective function* and Ω is the *constraint set* or *feasible region*. If $\Omega = \mathbf{R}^n$ the optimization problem is *unconstrained*, whereas $\Omega \subset \mathbf{R}^n$ makes the problem *constrained* to the region Ω .

A vector ϑ^* is a *local minimum* if it is not worse than its neighbors; that is, there is an $\varepsilon > 0$ such that

$$f(\vartheta^*) \leq f(\vartheta), \quad \forall \vartheta \in \Omega, \text{ with } \|\vartheta - \vartheta^*\| < \varepsilon \quad (3)$$

with $\|\cdot\|$ being the Euclidean l_2 -norm. On the other hand, a *global minimum* is a vector ϑ^* such that

$$f(\vartheta^*) \leq f(\vartheta), \quad \forall \vartheta \in \Omega \quad (4)$$

The local or global minimum is said to be *strict* if the inequalities in (3) and (4) are also strict for all $\vartheta \neq \vartheta^*$.

In order to minimize f and obtain a local or global minimum, optimization methods have to be used. Generally, an optimization method is an iterative process, which starts with an initial decision variable ϑ^0 (or an initial set of decision variables) and generates a sequence of ever-improving solutions $\vartheta^0, \dots, \vartheta^k$, by means of a given iterative rule. The iterative process stops when a convergence rule is satisfied. In the best case, this sequence converges towards the global minimum ϑ^* of f . In the worst case, the method can get trapped in a local minimum, having to be restarted in order to try to scape from it.

Depending on the nature of the objective function f different optimization methods can be applied. If f is continuous and differentiable, gradient based methods can be used. Classical algorithms of this type include the steepest descent method, the conjugate gradient method and the Newton's method [SY06]. But when the derivatives of the objective functions are unavailable, as in inverse reflector design, direct search methods fit as a good option [Rao96].

Pattern search is a subclass of these direct search algorithms, which involve the direct comparison of objective

function values and do not require the use of explicit or approximate derivatives. Torczon [Tor97] introduced the general class of pattern search methods for unconstrained optimization, demonstrating that the class of methods unified various distinct direct search techniques, such as the original pattern search of Hooke and Jeeves [HJ61], the Powell's method [Pow64], the Rosenbrock's method [Ros60] or the Simplex method [NM65].

4. The Inverse Design Method

Having so far established the definition of the optimization problem in Section 3, we can now reformulate it in terms of our inverse reflector design problem. Therefore, it can be stated as the minimization of an error metric (the objective function) between the irradiance distribution generated in a near field by a given reflector (the decision variable) and a desired near field irradiance distribution. In order to evaluate the actual irradiance distribution in the near field, and thus compute the value of the error metric, a modified global illumination light transport technique, called photon mapping, is used. A pattern search optimization algorithm is used in order to find the optimal reflector that minimizes de error metric.

4.1. The Decision Variable: NURBS Representation

NURBS have become the standard for curve and surface description in industry. We chose this representation for the reflector shape due to the fact that provide a unified mathematical basis for representing both analytic shapes (conic sections, quadric surfaces, etc.), as well as free-form entities such as reflector antennas, car bodies, ship hulls or aircraft fuselages [PT97]. On the other hand, NURBS also allows to specify and vary easily its continuity degree in order to meet the wide range of needs in the industrial design.

A p th-degree NURBS curve is defined by

$$C(u) = \frac{\sum_{i=0}^n N_{i,p}(u) w_i P_i}{\sum_{i=0}^n N_{i,p}(u) w_i} \quad a \leq u \leq b \quad (5)$$

where P_i are the *control points*, w_i are the *weights* and $N_{i,p}(u)$ are the p th-degree B-spline basis function defined on the non-periodic and non-uniform knot vector U [PT97].

We use a NURBS curve C to define a generatrix profile of a rotationally symmetric reflector R . In this way our method can define the shape of the reflector by moving the control points P_i and varying its weights w_i . Less control points defining the curve will represent a global shape for the reflector, whilst more control points will allow to make local modifications and introduce fine surface features. Due to the nature of the generatrix, control points are specified in 2D coordinates such that $P_i \equiv (x_i, y_i)$.

The optimization method specified in Section 4.5 governs

the shape of the reflector by means of the decision variable ϑ described in (2), and not directly handling the NURBS curve. Therefore, this decision variable is now stated as the sequence of control points and weights as follows

$$\vartheta \equiv (x_0, y_0, w_0, \dots, x_i, y_i, w_i, \dots, x_n, y_n, w_n) \quad (6)$$

therefore obtaining a decision variable ϑ in $\mathbf{R}^{3(n+1)}$. Using a NURBS curve with three control points (e.g. enough to define a conic section), the dimension of the optimization problem would be nine, whereas using directly a polygon mesh would make necessary a higher quantity of vertices.

The choice of a NURBS curve then reduces the dimension of the optimization problem, while gives more flexibility to the design of the surface.

4.2. The Near Field: Irradiance samples

The near field is that part of the space nearest to the reflector. Beyond the near field is the infinite far field. Therefore, while far field distributions, which assume a distant light source, are usually represented just in terms of angular variation, the near field representations adds spatial variation. We chose near field representation due to its real application: optical sets (generally a light source plus a reflector surface) are usually built in or hanged from ceilings or placed on pole-shaped supports, and generates a given light field on the floor and the surrounding area. Therefore, we can see the near field in our framework as the zone near the luminaire (floor, walls, road, etc.) where we want a desired light distribution.

We formally define the near field $F(R)$ as a set of points p_i uniformly distributed on a given surface S . At each point p_i , the incoming irradiance $E_i(R)$ due to the presence of the reflector R can be computed by means of the global illumination algorithm described in Section 4.4.

Therefore, in our framework, the near field can be either specified as a real 3D object with material properties, affecting to the inverse computation of the reflector, or it can be set as an invisible object, just registering the light that pass through. This aspect is important in our framework, because it allows to introduce a model of the environment where the luminaire is going to be finally placed, and thus optimize even more its behavior.

4.3. The Objective Function: RMS Error

To measure the fitness of the computed reflector an objective function has to be chosen. The objective function that we have used is the Root Mean Squared Error (RMSE) between the near field $F(R)$ generated by a reflector R and the desired irradiances in a near field $F(R^*)$. Therefore, the RMSE metric is expressed as follows

$$f(R) = RMSE(R) = \sqrt{\frac{\sum_{i=1}^N (E_i(R) - E_i(R^*))^2}{N}} \quad (7)$$

where $E_i(R^*)$ stands for the desired irradiance at the point p_i in the near field and N is the total number of points in the desired near field. The RMSE metric gives an idea of the mean deviation of the irradiance samples in the near field in irradiance units (W/m^2).

4.4. The Simulation: Photon Mapping

In order to compute the irradiance distribution arriving to the near field, we use the traditional photon mapping algorithm [Jen01] with a modification on the storing process of photons. The photon mapping algorithm is a two-pass method. First, photons are traced from light through the scene, storing each interaction in a special *k nearest neighbor* (k-NN) structure totally decoupled from the geometry, called *photon map*. Second, irradiance estimates are performed using density estimation techniques on the photon map.

Using photon mapping has the advantage that the error in the estimation of the irradiance is of low frequency (bias) rather than the high frequency noise (variance) in Monte Carlo ray tracing. Other advantages of using photon mapping include using arbitrary complex geometry and BRDFs for the reflector surface. The photon mapping algorithm also makes possible the accurate computation of caustic effects due to the reflection of light in specular surfaces, such as the case of a reflector surface. Finally, this rendering algorithm allows to simulate inter-reflections in the bounding volume of the reflector surface. In this manner, the photon mapping offers to our framework a full global solution of the light distribution generated by the presence of a reflector.

The outline of the behavior of the photon algorithm in our framework is as follows:

- Stage 1: Photon Tracing
 - Photons are emitted from a diffuse point light of power Φ . Each photon carries a part of that power. Again, arbitrary complex light sources could be used using specific sampling techniques. In scenes with sparse geometry, such as the one treated in this paper, many photons do not hit any object. In order to reduce this waste of time, we use projection maps [JC95]. In that way, all the emitted photons are directed towards the reflector surface.
 - Photons are traced through the scene in the same way as ray tracing. When a photon interacts with a surface, it can be either absorbed, reflected or transmitted. This is done statistically, based on the material properties of the reflector by means of the Russian Roulette technique [BES96].

- The original algorithm stores the photons in the photon map structure whenever an interaction happens. In our method, only photons interacting with the near field are important. Therefore, as a modification of the original photon mapping algorithm, we only store photons that hit or go through the near field studied, after interacting with the reflector. In that sense we can store more photons in the photon map in order to compute more accurate irradiance estimates in the near field.

- Stage 2: Irradiance Estimate

- To compute the irradiances values along the near field, the algorithm perform a irradiance estimate at each point p_i on the near field. An irradiance estimate is a density estimate, such that

$$E_i = \frac{1}{\pi r^2} \sum_{j=1}^N K(\|p_i - ph_j\|) \Phi_j \quad (8)$$

where K is a *kernel* used to weight the flux contributions Φ_j from each photon based on their distance to the point p_i . N is the number of photons used to compute the estimate and is also called the *bandwidth*, and r is the radius of the bounding sphere including the N photons of the estimate.

Increasing the bandwidth of the kernel, the variance is reduced, but the bias is increased in the irradiance estimation, blurring highlights and caustics. This artifact is not desirable in our simulation, due to the intrinsic connection between caustics and the ever-present curvature of the reflector surfaces [MH92]. In order to cushion this increasing bias we use the Silverman kernel [SWH*95], which has a better behavior than others widespread kernels [Sch03].

4.5. The Optimization Method: Hooke and Jeeves

Recalling (2), *Direct Search* methods are optimization algorithms that neither compute or explicitly approximate derivatives of f in order to minimize it. Pattern search methods are included in this latter group, and the common behavior is that they use a pattern of points that is independent of the objective function f .

Torczon introduced in [Tor97] the general class of *Pattern Search* optimization methods, where the method which we use, developed by Hooke and Jeeves [HJ61], is included. Torczon introduced generalizations to define important concepts common to all pattern search methods, such as *pattern*, *exploratory move* and the search method itself. Furthermore, in her work proposes a detailed global convergence theory [Tor97].

Among all of existing pattern search methods we select the original local search algorithm of Hooke and Jeeves [HJ61], due to its simplicity. The Hooke-Jeeves algorithm is a variant of the *Coordinate Search*, first described by

Davidon [Dav91], which incorporates a *pattern step* in order to accelerate the search process from previous successful movements, in an opportunistic way.

The Hooke-Jeeves starts with an initial guess decision variable ϑ^0 and a real valued step size Δ , and iteratively found ever-improving solutions by sequencing an exploratory step [Dav91] and a pattern step.

4.5.1. Exploratory step: Coordinate Search

The coordinate search step performs exploratory moves around a base point ϑ^k , finding new trial points by using a real valued step Δ , getting at the end a new point ϑ^{k+1} . Given a trial point $\vartheta^{k+1} \equiv (\vartheta_1, \dots, \vartheta_i, \dots, \vartheta_n)$ two exploratory moves are defined for each coordinate i from 1 to n

$$\vartheta_{i+}^k \equiv (\vartheta_1, \dots, \vartheta_i + \Delta, \dots, \vartheta_n) \quad (9)$$

$$\vartheta_{i-}^k \equiv (\vartheta_1, \dots, \vartheta_i - \Delta, \dots, \vartheta_n) \quad (10)$$

The coordinate search starts the process by performing the exploratory moves on $\vartheta^{k+1} = \vartheta^k$, first ϑ_{i+}^{k+1} , and then ϑ_{i-}^{k+1} , on coordinate $i = 1$. The first successful move update the new trial point ϑ^{k+1} . So, if $f(\vartheta_{i+}^{k+1}) < f(\vartheta^{k+1})$ then $\vartheta^{k+1} = \vartheta_{i+}^{k+1}$, whilst if $f(\vartheta_{i-}^{k+1}) < f(\vartheta^{k+1})$ then $\vartheta^{k+1} = \vartheta_{i-}^{k+1}$. If neither of them success then ϑ^{k+1} is not updated. After that, this process is again repeated for coordinate $i + 1$, starting with the new trial point ϑ^{k+1} . In the best case, and after iterating over all the n coordinates, the exploratory step returns a point $\vartheta^{k+1} \neq \vartheta^k$ which assures that $f(\vartheta^{k+1}) < f(\vartheta^k)$. In the worst case, the point ϑ^{k+1} is the same as the starting point ϑ^k , after $2n$ trial points were evaluated.

4.5.2. Pattern Step

The main idea of the pattern step is to investigate whether further progress is possible in the main promising direction. This assumption, let the algorithm advance faster, hopefully towards the global minimum, avoiding some extra expensive evaluations of the objective function.

Given iterates ϑ^{k-1} and ϑ^k , the pattern step performs an evaluation of f at $a^k = \vartheta^k + \alpha(\vartheta^k - \vartheta^{k-1})$, with α as an acceleration factor. The trial point a^k is temporarily accepted, even if $f(a^k) \geq f(\vartheta^k)$. The algorithm performs then a coordinate search around the trial point a^k . If the coordinate search succeeds, then the point returned is accepted as the new iterate ϑ^{k+1} . If not, the algorithm compute a new coordinate search around ϑ^k . If the latter fails again, the step Δ is reduced for the next iteration.

5. Results

We have tested our framework with a theoretical known solution: the light distribution produced by a paraboloid reflector. The paraboloid is the rotationally symmetric surface

generated by a half-parabola (a kind of conic section). In our test problem we define the half-parabola as follows

$$R_{par}(t) = (2at, a(1-t^2)+h) \quad t \geq 0, a > 0, h > 0 \quad (11)$$

where a stands for the distance between the focus and the vertex of the parabola and h is the distance between the focus and the desired near field.

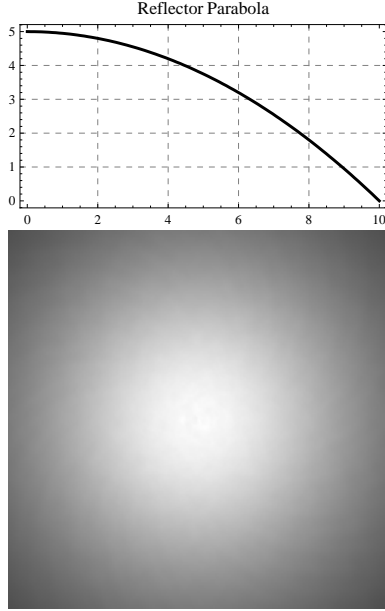


Figure 1: The parabolic reflector. Top: the NURBS curve generatrix. Bottom: the desired irradiance distribution on the near field.

The parabola has two main interesting optical features [BW86]. First, rays emitted from its focus are reflected in a parallel way (e.g. perpendicular to the near field). Second, a spherical wavefront emitted from the focus, is reflected as a planar wavefront. Therefore, if we place a diffuse light source in the focus of the parabola defined in (11), we can express the irradiance E_i^I arriving to a point p_i in a near field at a distance h from the focus, and after a reflection in the surface, as follows

$$E_i^I = \frac{\Phi}{4\pi a^2 \left(1 + \frac{\|p_i\|^2}{4a^2}\right)^2} \quad (12)$$

where Φ is the power of the diffuse light source and $\|p_i\|$ is the distance between the point p_i and the focus, projected into the near field. On the other hand, the irradiance E_i^D that directly comes from the light source (without any previous reflection) is stated as

$$E_i^D = \frac{\Phi}{4\pi h^2} \left(\frac{1}{\sqrt{1 + \frac{\|p_i\|^2}{h^2}}}\right)^3 \quad (13)$$

We can now add (12) and (13) in order to compute the total irradiance E_i that arrives to the near field due to direct and indirect illumination.

In our results we performed an inverse design of a paraboloid reflector with $a = 5\text{ cm}$. In order to enforce the near field based design of the reflector we chose a value of 5 cm for the distance h between the light source and the near field. Such configuration produce a maximum irradiance of 2 W/m^2 just in the near field point below the light source. Figure 1 shows the parabola along with the desired near field. The selected parabola can be modeled as a NURBS curve with control points $P_0 = (0, a+h)$, $P_1 = (a, a+h)$ and $P_2 = (2a, h)$, and weights w_0 , w_1 and w_2 with value 1.

In order to run the inverse design, an initial reflector has to be determined as input to the optimization algorithm. Figure 2 shows the three initial reflectors selected, named reflectors A, B and C. Figure 3 shows three views of the objective function RMSE, marked with the initial errors of the reflectors A, B and C, and the global minimum P (the parabolic reflector). As we stated in Section 4.1, all reflectors are designed and handled by means of a NURBS curve via the decision variable ϑ . In our tests we define all the reflectors just like the objective parabola: a NURBS curve with three control points (and a weight for each one). Therefore the problem has dimension nine, but we fix seven of them to their final values, reducing the optimization problem to the \mathbf{R}^2 space. The decision variable is then $\vartheta = (w_1, x_2)$, where w_1 is the weight of the control point P_1 and x_2 is the x coordinate of the control point P_2 . The initial decision variable for reflector A is $\vartheta^0 = (1.6, 9)$, for B is $\vartheta^0 = (1.8, 7)$ and for C is $\vartheta^0 = (\sqrt{2}/2, 5)$ (hemi-spheric reflector).

We performed eight tests with the three latter reflectors varying two parameters of the Hooke-Jeeves algorithm: the step size Δ and the acceleration factor α . Table 2 shows the optimal reflectors ϑ^* obtained for each test. Figure 4 shows the sequences of the ever-improving solutions on a contour-line plot of the RMSE function to optimize.

From these results it can be seen that when the initial reflector ϑ^0 is in the concave region of the global minimum $\vartheta^* = (1, 10)$, the algorithm converges towards ϑ^* , independently of the parameters Δ and α (reflector A). In other cases, like the reflector B, a fine tuning of the initial step size Δ has to be performed, in order to not fall in a local minimum. Extreme cases, like the hemi-spheric reflector C, are not able to scape from deep local minima due to its surrounding orography.

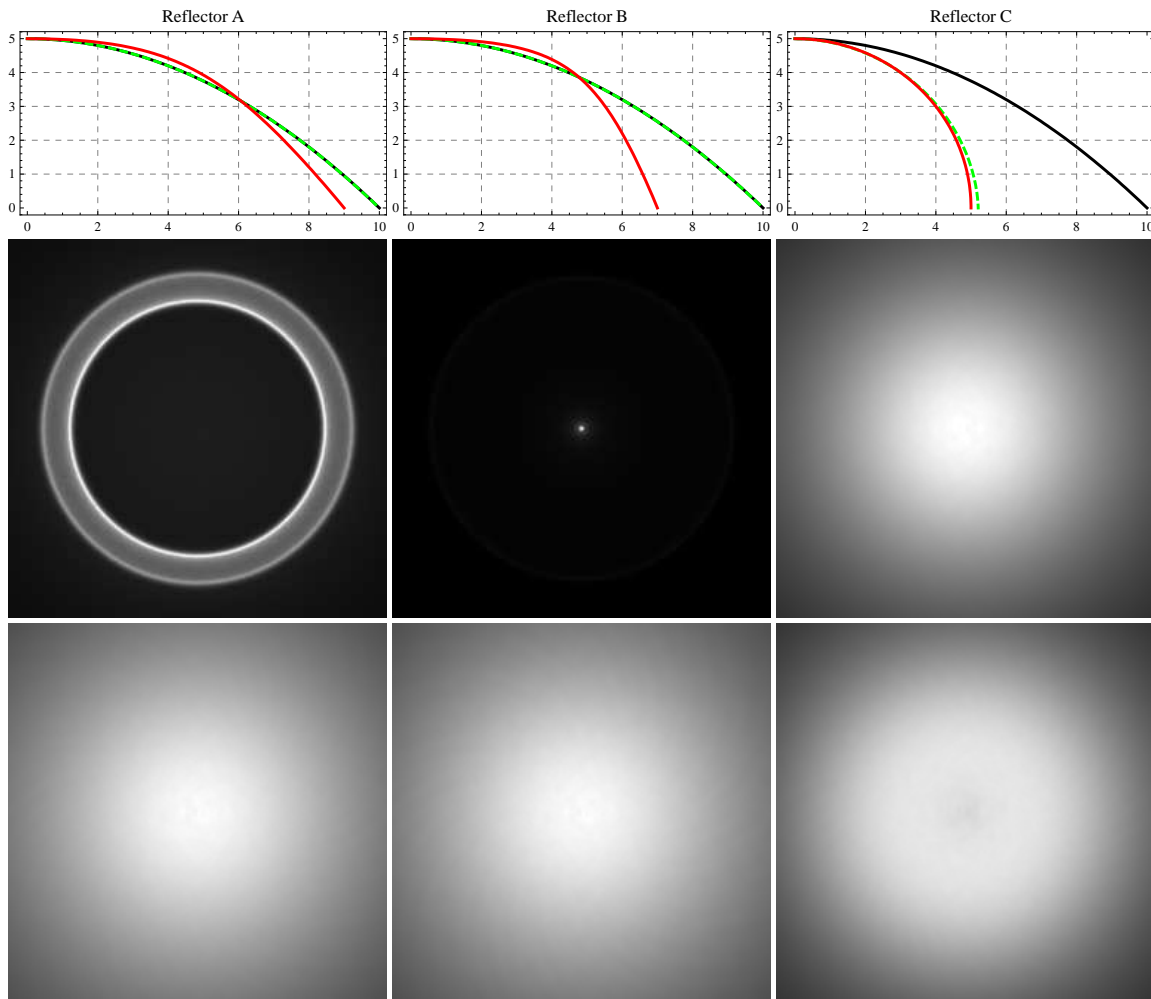


Figure 2: Initial reflectors A, B and C for the tests in Table 2. Top: The NURBS curves of initial reflectors A, B and C (red lines), compared with the desired parabola (black lines) and the obtained reflector (dashed green lines). Middle: the irradiance distribution generated by these initial reflectors in the near field. Bottom: the irradiance distribution generated by the obtained reflectors.

6. Conclusions

We have presented a comprehensive framework for inverse designing rotationally symmetric reflectors given a desired near field of irradiances distribution.

We use a NURBS curve to represent the generatrix of the reflector surface. In this sense, we reduce the dimension of the optimization problem, overcoming the problem present in polygon based works [PPV04]. Additionally, the use of NURBS, instead of other Spline approaches [Neu94], gives more flexibility to the design process.

For the simulation stage, a modified photon mapping technique is applied. The original algorithm [Jen01] gives a full global solution to the light interaction with the reflector,

while our modification in the photon storing process only registers the particles that interact with the near field, saving memory space and giving more accuracy in the irradiance estimate. As opposed to other works this is done in three dimensional space [DCC99]. The specification of the near field is general enough to represent the environment close to the reflector, such as floor, walls, etc.

Finally, the strategy chosen to perform the optimization of the selected RMSE function as objective function is the Hooke-Jeeves algorithm [HJ61]. This algorithm, based in exploratory moves and optimistic progression, achieves good results if the initial reflector belongs to a moderately convex zone of the RMSE function, regardless of the dimensionality of the problem.

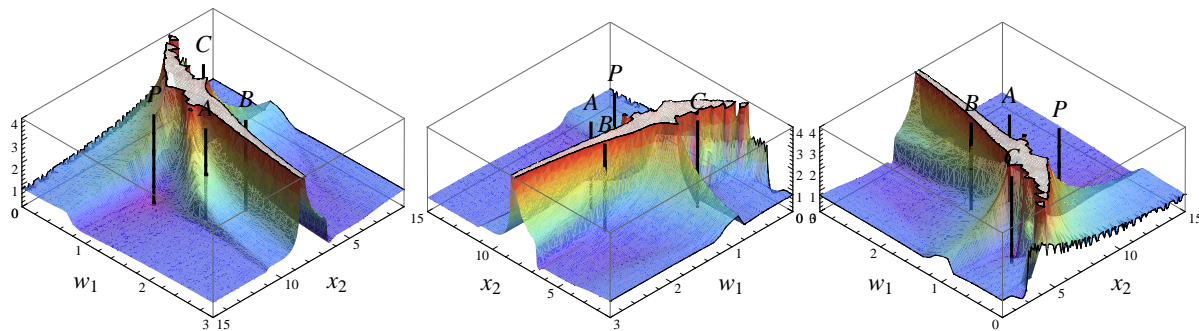


Figure 3: Several views of the RMSE function in the surrounding area of the global minimum given by the parabolic reflector P , showing the error of the initial reflectors A , B and C . For the sake of clarity, only the range of values between 0 and 4 of the RMSE function is shown.

Table 2: Comparative results for several tests performed on initial reflectors A , B and C (see Figure 2). Starting step size Δ has a value of 1 cm for coordinate x_2 and 0.5 for weight w_1 . The acceleration factor α has a value of 1. ϑ^0 is the decision variable for the initial reflector, ϑ^* is the optimal reflector computed, $RMSE(\vartheta^*)$ is the fitness value of the optimal reflector ϑ^* , k stands for the number of iterates in the sequence $\vartheta^0, \dots, \vartheta^k$.

	Refl.	Step size	Acceleration	$\vartheta^0 \equiv (w_1, x_2)$	$\vartheta^* \equiv (w_1, x_2)$	$RMSE(\vartheta^*)$	k	iterations	time
1	A	Δ	α	(1.6, 9)	(1, 9.99668)	0.00343334	14	25	17m 25s
2	A	2Δ	α	(1.6, 9)	(1, 9.99844)	0.00404593	10	20	15m 55s
3	A	$\Delta/2$	α	(1.6, 9)	(1.00094, 10.0002)	0.00405967	23	33	27m 08s
4	A	Δ	2α	(1.6, 9)	(0.999999, 10.0336)	0.00896852	9	19	15m 01s
5	A	Δ	$\alpha/2$	(1.6, 9)	(1.00125, 9.99141)	0.00437376	12	23	16m 32s
6	B	Δ	α	(1.8, 7)	(2.28375, 4.8125)	0.403432	8	18	14m 16s
7	B	2Δ	α	(1.8, 7)	(1.00125, 9.99687)	0.00445291	18	28	23m 01s
8	C	Δ	α	$(\sqrt{2}/2, 5)$	(0.689429, 5.20508)	0.0878155	5	15	12m 17s

7. Future Work

A deeper observation has to be performed in the connection between the topology of the surface (curvature, orientation, etc.) and the irradiances generated at the near field. That fact can give us some clues about a good heuristic to direct the optimization process. In this sense, other kind of decision variables could feed the inverse design, based on curvatures instead of moving control points and weights.

Other alternatives to the Hooke-Jeeves algorithm can be taken into account, such as Evolutionary Strategies and Genetics Algorithms [Bäc95], or other heuristics such as Simulated Annealing [KGV83] or Particle Swarm [KE95]. Together with the study of other optimization methods, new error metrics and distance function could be studied in order to model the objective function.

In the simulation process, the irradiance estimate is crucial to get a physically based approach in order to meet the industry needs. In this sense, approaches such as the work of Schregle [Sch03] can be very interesting in order to reduce bias and variance in the density estimation.

Although our problem is stated in terms of inverse geometry, the generality of our model would allow an extension

for the recovery of an unknown BRDF or the resolution of an inverse lighting problem. Additionally, cases based on industrial reflector design have to be tested along with other academic examples, as the one presented in this paper.

8. Acknowledgements

We thank the anonymous reviewers for their valuable comments. This research has been funded by the projects TIN2007-63025 (Spanish Ministry of Science and Technology) and UZ2007-TEC06 (University of Zaragoza). Diego Gutierrez was additionally supported by a mobility grant by the Gobierno de Aragón (Ref: MI019/2007).

References

- [Arv95] ARVO J. R.: *Analytic Methods for Simulated Light Transport*. PhD thesis, Yale University, 1995.
- [Bäc95] BÄCK T.: *Evolutionary Algorithms in Theory and Practice: Evolution Strategies, Evolutionary Programming, Genetic Algorithms*. Oxford University Press, 1995.

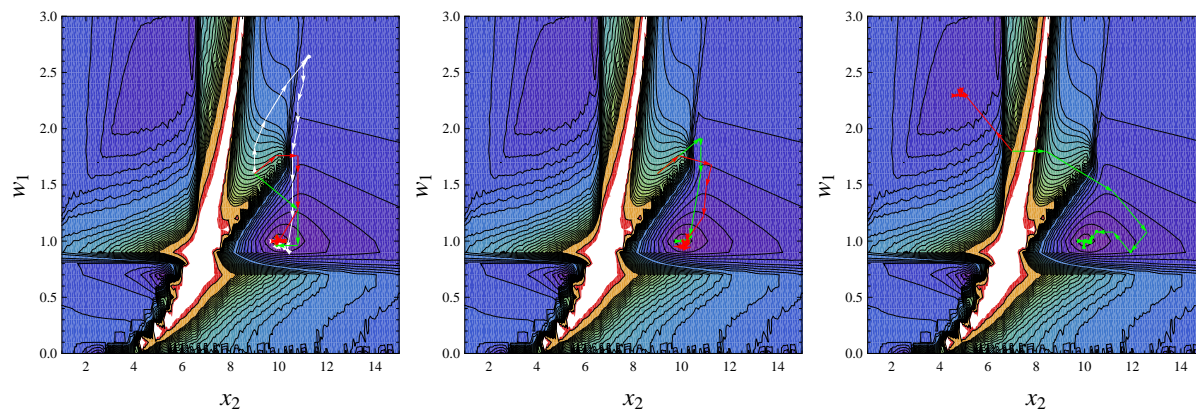


Figure 4: The behavior of the Hooke-Jeeves algorithm when varying the step size Δ and the acceleration factor α , showing the sequences of ever-improving solutions $\vartheta^0, \dots, \vartheta^k$ for several tests in Table 2. The three contour plots represent the RMSE function in Figure 3. Left, initial reflector A: Sequences for tests 1, 2 and 3 (Red, Green and White, respectively). Center, initial reflector B: Sequences for tests 4 and 5 (Green and Red, respectively). Right, initial reflector C: Sequences for tests 6 and 7 (Red and Green, respectively).

- [BES96] BLOM G., ENGLUND J.-E., SANDELL D.: General russian roulette. *Mathematics Magazine* 69, 4 (October 1996), 293–297.
- [BW86] BORN M., WOLF E.: *Principles of Optics: Electromagnetic Theory of Propagation, Interference and Diffraction of Light*, 6th ed. Cambridge University Press, October 1986.
- [CKP*07] CHOI A.-S., KIM C.-H., PARK B.-C., SONG K.-D., KIM Y.-S.: Preliminary study on luminous intensity distribution modeling of the dome pendent prismatic luminaire and application of optimization techniques. *Building and Environment* 42 (2007), 1173–1182.
- [Dav91] DAVIDON W. C.: Variable metric method for minimization. *SIAM Journal on Optimization* 1 (1991), 1–17.
- [DCC99] DOYLE S., CORCORAN D., CONELL J.: Automated mirror design using an evolution strategy. *Optical Engineering* 38, 2 (1999), 323–333.
- [DHS*05] DURAND F., HOLZSCHUCH N., SOLER C., CHAN E., SILLION F. X.: A frequency analysis of light transport. *ACM Transactions on Graphics* 24, 3 (2005), 1115–1126.
- [HJ61] HOOKE R., JEEVES T. A.: “direct search” solution of numerical and statistical problems. *Journal of the ACM* 8, 2 (1961), 212–229.
- [JC95] JENSEN H. W., CHRISTENSEN N. J.: Photon maps in bidirectional monte carlo ray tracing of complex objects. *Computers & Graphics* 19, 2 (1995), 215–224.
- [Jen01] JENSEN H. W.: *Realistic image synthesis using photon mapping*. A. K. Peters, Ltd., Natick, MA, USA, 2001.
- [Kaj86] KAJIYA J. T.: The rendering equation. *ACM SIGGRAPH Computer Graphics* 20, 4 (1986), 143–150.
- [KE95] KENNEDY J., EBERHART R. C.: Particle swarm optimization. In *Proceedings of IEEE International Conference on Neural Networks* (1995), pp. 1942–1948.
- [KGV83] KIRKPATRICK S., GELATT C. D., VECCHI M. P.: Optimization by simulated annealing. *Science* 220, 4598 (May 1983), 671–680.
- [LJPP06] LOSCOS C., JACOBS K., PATOW G., PUEYO X.: Inverse rendering: From concept to applications. In *Eurographics 2006: Tutorials* (2006), Eurographics Association, pp. 399–547.
- [Mar98] MARSCHNER S.: *Inverse Rendering for Computer Graphics*. PhD thesis, Cornell University, 1998.
- [MG97] MARSCHNER S. R., GREENBERG D. P.: Inverse lighting for photography. In *Proceedings of the Fifth Color Imaging Conference, Society for Imaging Science and Technology* (1997).
- [MH92] MITCHELL D., HANRAHAN P.: Illumination from curved reflectors. *ACM SIGGRAPH Computer Graphics* 26, 2 (1992), 283–291.
- [Neu94] NEUBAUER A.: The iterative solution of a nonlinear inverse problem from industry: design of reflectors. In *Proceedings of the international conference on Curves and surfaces in geometric design* (1994), A. K. Peters, Ltd., pp. 335–342.
- [NM65] NELDER J. A., MEAD R.: A simplex method for function minimization. *Computer Journal* 7 (1965), 308.
- [Oli08] OLIKER V. I.: A minkowski-style theorem for focal functions of compact convex reflectors. *Transactions*

- of the American Mathematical Society 360, 2 (February 2008), 563–574.
- [Pow64] POWELL M. J. D.: An efficient method for finding the minimum of a function of several variables without calculating derivatives. *Computer Journal* 7, 4 (1964), 303–307.
- [PP03] PATOW G., PUEYO X.: A survey of inverse rendering problems. *Computers & Graphics* 22, 4 (2003), 663–687.
- [PPV04] PATOW G., PUEYO X., VINACUA A.: Reflector design from radiance distributions. *International Journal of Shape Modeling* 10, 2 (2004), 211–236.
- [PT97] PIEGL L., TILLER W.: *The NURBS Book*, 2nd ed. Monographs in Visual Communication. Springer, 1997.
- [Rao96] RAO S. S.: *Engineering Optimization: Theory and Practice*, 3rd ed. Wiley, 1996.
- [RH01] RAMAMOORTHI R., HANRAHAN P.: An efficient representation for irradiance environment maps. In *SIGGRAPH '01: Proceedings of the 28th annual conference on Computer graphics and interactive techniques* (New York, NY, USA, 2001), ACM, pp. 497–500.
- [Ros60] ROSENBROCK H. H.: An automatic method for finding the greatest or least value of a function. *Computer Journal* 3, 3 (1960), 175–184.
- [Sch03] SCHREGLE R.: Bias compensation for photon maps. *Computer Graphics Forum* 22, 4 (2003), 729–742.
- [SWH*95] SHIRLEY P., WADE B., HUBBARD P. M., ZARESKI D., WALTER B., GREENBERG D. P.: Global illumination via density estimation. In *Rendering Techniques '95 (Proceedings of the Sixth Eurographics Workshop on Rendering)* (New York, NY, 1995), Hanrahan P. M., Purgathofer W., (Eds.), Springer-Verlag, pp. 219–230.
- [SY06] SUN W., YUAN Y. X.: *Optimization Theory and Methods, Nonlinear Programming*, vol. 1 of *Springer Optimization and Its Applications*. Springer, 2006.
- [Tor97] TORCZON V.: On the convergence of pattern search algorithms. *SIAM Journal on Optimization* 7, 1 (1997), 1–25.
- [Wan96] WANG X. J.: On the design of a reflector antenna. *Inverse Problems* 12 (1996), 351–375.
- [WN75] WESTCOTT B. S., NORRIS A. P.: Reflector synthesis for generalized far-fields. *Journal of Physics A: Mathematical and General* 8, 4 (1975), 521–532.